The inflammatory response of the supraspinatus muscle in rotator cuff tear conditions

Frich, Lars Henrik; Fernandes, Livia Rosa; Schrøder, Henrik Daa; Hejbøl, Eva Kildall; Nielsen, Pernille Vinther; Jørgensen, Puk Hvirgel; Stensballe, Allan; Lambertsen, Kate Lykke

Published in:
Journal of Shoulder and Elbow Surgery

DOI (link to publication from Publisher):
10.1016/j.jse.2020.08.028

Publication date:
2020

Document Version
Version created as part of publication process; publisher's layout; not normally made publicly available

Journal Pre-proof

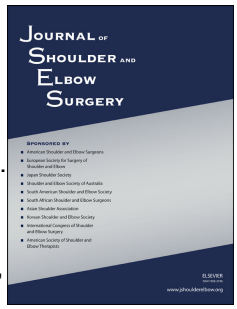

The inflammatory response of the supraspinatus muscle in rotator cuff tear conditions.

Lars Henrik Frich, MD, PhD, Livia Rosa Fernandes, PhD, Henrik Daa Schrøder, DMSc, Eva Kildall Hejbøl, PhD, Pernille Vinther Nielsen, BSc, Puk Hvirgel Jørgensen, MSc, Allan Stensballe, PhD, Kate Lykke Lambertsen, PhD

PII: S1058-2746(20)30710-2

DOI: https://doi.org/10.1016/j.jse.2020.08.028

Reference: YMSE 5352

To appear in: *Journal of Shoulder and Elbow Surgery*

Received Date: 24 April 2020

Revised Date: 14 August 2020

Accepted Date: 17 August 2020

Please cite this article as: Frich LH, Fernandes LR, Schrøder HD, Hejbøl EK, Nielsen PV, Jørgensen PH, Stensballe A, Lambertsen KL, The inflammatory response of the supraspinatus muscle in rotator cuff tear conditions., *Journal of Shoulder and Elbow Surgery* (2020), doi: https://doi.org/10.1016/j.jse.2020.08.028.

The inflammatory response of the supraspinatus muscle in rotator cuff tear conditions.

Lars Henrik Frich, MD, PhD[1,2,3*], Livia Rosa Fernandes, PhD[4], Henrik Daa Schrøder, DMSc[5], Eva Kildall Hejbøl, PhD[5], Pernille Vinther Nielsen, BSc[2], Puk Hvirgel Jørgensen, MSc[6], Allan Stensballe, PhD[6], Kate Lykke Lambertsen, PhD[4,7,8]

[1] Department of Orthopaedics, Odense University Hospital. Odense, Denmark

[2] The Orthopaedic Research Unit, University of Southern Denmark, Odense, Denmark

[3] Institute of Molecular Medicine, University of Southern Denmark, Odense, Denmark,

[4] Department of Neurobiology Research, Institute of Molecular Medicine, University of Southern Denmark, Odense, Denmark,

[5] Department of Pathology, Odense University Hospital, Odense, Denmark

[6] Department of Health Science and Technology, Aalborg University, Aalborg, Denmark

[7] Department of Neurology, Odense University Hospital, Odense, Denmark

[8] BRIDGE – Brain Research – Inter-Disciplinary Guided Excellence, University of Southern Denmark, Odense, Denmark

***Corresponding author:** Lars Henrik Frich, lars.henrik.frich@rsyd.dk, J.B. Winsloewsvej 4, DK-5000 Odense C, Denmark.

Running title: Muscle inflammation and rotator cuff

Conflicts of interest: None

Acknowledgments

Ulla Damgaard Munk and Anni Petersen are acknowledged for skilled technical assistance. Peter Gaster and Søren Skødt Kristensen are acknowledged for their assistance with collecting tissue biopsies. Claire Gudex is acknowledged for proofreading.

Funding

We acknowledge the generous funding from the Danish Rheumatism Association (R150-A4380) and Odense University Hospital Research Fund (A3159). The Danish National Mass Spectrometry Platform for Functional Proteomics (PRO-MS: grant no. 5072-00007B) and the Svend Andersen Foundation are acknowledged for parts of this study.

Ethics

Ethical approval was granted by The Regional Committees on Health Research Ethics for Southern Denmark, J. No. S-20160037, and the study reported to The Danish Data Protection Agency (16/9714). The project was approved by the Orthopedic Research Board, Odense University Hospital.

The inflammatory response of the supraspinatus muscle in rotator cuff tear conditions.

Running title: Muscle inflammation and rotator cuff

Abstract

Background: Rotator cuff (RC) disorders involve a spectrum of shoulder conditions from early tendinopathy to full-thickness tears leading to impaired shoulder function and pain. The pathology of RC disorder is, nonetheless, still largely unknown. It is our hypothesis that supraspinatus (SS) tendon tear leads to sustained inflammatory changes of the SS muscle along with fatty infiltration and muscle degeneration, which are threshold markers for poor RC muscle function. The aim of this study was to determine the extent of this muscle inflammation in conjunction with lipid accumulation and fibrosis in RC tear conditions.

Methods: We used proteomics, histology, electrochemiluminescence immunoassay, and qPCR analyses to evaluate inflammatory and degenerative markers and fatty infiltration in biopsies from 22 patients undergoing surgery with repair of a full- thickness supraspinatus (SS) tendon tear.

Results: Bioinformatic analysis showed that proteins involved in innate immunity, extracellular matrix organization, and lipid metabolism were among the most upregulated whereas mitochondrial electronic transport chain along with muscle fiber function were among the most downregulated. Histological analysis confirmed changes in muscle fiber organization and the presence of inflammation and fatty infiltration. Inflammation appeared to be driven by a high number of infiltrating macrophages, accompanied by elevated matrix metalloprotease levels and changes in transforming growth factor-β and cytokine levels in the SS compared to the deltoid muscle.

Conclusions: We demonstrated massive SS muscle inflammation after tendon tear combined with fatty infiltration and degeneration. The regulation of tissue repair is thus extremely complex, and it may have opposite effects at different time points of healing. Inhibition or stimulation of muscle inflammation may be a potential target to enhance outcome of the repaired torn RC.

Level of evidence: Basic Science Study; Histology, Molcular and Cell Biology

Keywords: Shoulder disorder, muscle damage, proteomics, protein changes, extracellular matrix degeneration, fatty infiltration

Introduction

Rotator cuff (RC) lesions are some of the most common shoulder conditions in humans and can lead to weakness, pain, and limited/reduced mobility. The prevalence of RC tears is age-dependent, and both partial and full-thickness RC tears increase markedly after 50 years of age [48]. The etiology of RC diseases is multifactorial with frequent involvement of the supraspinatus (SS) tendon [5]. Full-thickness SS tears do not heal spontaneously, and surgically repaired RC tears tend to heal poorly [15; 33]. A recent Cochrane review questioned whether repair of RC tears provides meaningful benefit to patients with symptomatic RC tears [24]. There is, therefore, a pressing need to better understand the pathophysiology behind RC tear conditions in order to improve results after surgical repair of RC tendon tears.

In full-thickness RC tears, increased numbers of immune cells have been demonstrated in the synovial tissue adjacent to the SS tendon [1] and an increase in tear size correlated with a greater pro-inflammatory response in the synovium [6; 45]. Recent data suggest that the RC muscles also become inflamed in the presence of an RC tear [14], and results from experimental models suggest that acute inflammation plays a detrimental role in the onset of chronic muscle damage following RC tears [16; 29]. It is also generally agreed that chronic RC tendon lesion leads to degenerative muscle changes in the form of fatty infiltration and fibrosis [10].

Several animal studies have provided evidence of significant increases in inflammatory cytokines, growth factors, and matrix metalloproteases (MMPs), indicating muscle inflammation following experimental RC tendon tear [16; 29]. Changes in the biology of human RC muscles in tear conditions

remain poorly defined at the cellular level, however, and RC muscle as a target for inflammation following RC tear is only sparsely understood [14; 23].

The aim of this study was to provide a more robust understanding of the inflammatory environment of human SS muscle in RC tear conditions. It is our hypothesis that inflammatory conditions precede disturbances of the muscle architecture, and eventually lead to RC muscle fatty infiltration and degeneration. To investigate this, we applied quantitative proteomics followed by histological, multiplex chemiluminescence, and qPCR analyses of inflammation in SS and deltoid muscle biopsies that were harvested from patients undergoing surgery for RC tears.

Materials and methods

Patient cohort

Patients (n=22) with a relevant shoulder trauma and clinical signs of an RC lesion were recruited (Supplementary Table 1). Median age of lesions was 3.3 months (IQR 2-14 months). Patients underwent preoperative magnetic resonance imaging scan revealing SS tendon tear, and all tears were confirmed at surgery. Informed written consent was obtained from all patients. The workflow of the project is presented in Figure 1.

Human tissue

The RC and musculotendinous junction of the SS muscle were gently débrided from fascia and bursal tissue using a blunt shaver. SS tendon and muscle biopsies were harvested from the edge of the tendon and approximately one centimeter medial to the tendon, respectively, under direct visualization from the arthroscope. Comparative biopsies were taken from assumed healthy, ipsilateral deltoid muscles. Biopsies were snap-frozen on dry ice and stored at -80°C or fixed in 10% neutral buffered formalin and embedded in paraffin.

Blood samples

Blood samples were obtained in EDTA coated test tubes immediately prior to surgery to estimate preoperative peripheral inflammation. Hemoglobin, C-reactive protein and white blood cell counts were analyzed. The patient cohort was also tested for presence of rheumatic factors (anti-nuclear, anti-cyclic citrullinated, and mitochondrial antibodies and rheumafactor).

Histology and Immunohistochemistry

SS or deltoid muscle tissue was sectioned into 2μm thick sections on a microtome. Immunohistochemistry for CD68 was performed on the OMNIS platform (Dako/Agilent, Denmark) using mouse anti-CD68 (1:50, Clone PG-M1) antibody and EnVision™ FLEX as detection system, while immunohistochemistry for FOXP3, CD3, and adipophilin was performed on a BenchMark Ultra immunostainer (Ventana Medical Systems, AZ, USA) using mouse anti-FOXP3 (1:40, clone 236A/E7), rabbit anti-CD3 ("*ready-to-use*", clone 2GV6), and mouse anti-adipophilin (1:50, clone AP125) antibodies and the OptiView-DAB detection system. Parallel sections were stained with hematoxylin and eosin (HE).

Slides were scanned on a NanoZoomer 2.0 RS scanner (Hamamatsu Photonics, Visiopharm, Denmark). To produce merged images, NDP view (Hamamatsu Photonics, version 2.6.17) was applied to find identical regions on neighboring cells stained for FOXP3 and CD3, respectively. The images were processed and merged using Photoshop C6 (Adobe Systems, CA, USA) and ImageJ/Fiji. The area with muscle tissue in each biopsy was determined using the freehand region function and the number of CD3 and FOXP3 within this area was manually counted at 20x magnification.

Proteomics

Homogenization of tissue biopsies

Approximately 1mm^3 was cut from the frozen tendon and muscle biopsies and was homogenized by bead beating using ss 0.9-2.0mm beads (Bullet blender Gold, Next Advance Inc, USA) in reducing lysis buffer (5% sodium deoxycholate (SDC; Sigma Aldrich, USA), protease inhibitors (cOmplete, Roche) in 50mM TEAB (Sigma Aldrich). Protein concentration in lysates was determined by protein A280 and lysates stored at -80ºC (DeNoviX, USA).

Samples were further processed using an optimized SDC filter-aided sample preparation protein digestion (SDC-FASP) essentially as [4] using 100µg protein starting material in 10kDa molecular weight cutoff spin-filters (Merch Millipore, Singapore). The lysates were reduced (10mM TCEP) and alkylated (50mM Chloroacetamide) each for 15min in digestion buffer (5% SDC in 50mM TEAB; Sigma-Aldrich). Overnight trypsin digestion at 37°C was performed by addition of 200µl 0.5% digestion buffer containing Trypsin 1:50 (v:v; Pierce, USA). Peptides were extracted by acidification and phase-separation, where 3:1 (v/v) ethyl acetate of sample volume was added and acidified by adding Trifluoroacetic acid (Sigma-Aldrich) to a final concentration of 1% (pH<2) followed by centrifigation. The collected lower aqueous phase containing the peptides was dried in a vacuum centrifuge and dissolved in 0.1M TEAB. Peptide concentration in lysates was determined by protein A280 and lysates stored at -80ºC (DeNoviX, USA).

iTRAQ labeling

A total of 5µg of each sample was labeled with a 4-plex iTRAQ kit (AB Sciex, USA) according to manufacturer's instructions. Briefly, samples were re-dissolved to total volume of 25µL 0.1M TEAB, pH 8.5 while 290µL 96% ethanol were added to iTRAQ reagents. Next, 50µL of the iTRAQ reagents was transferred to the samples, which were then labelled, mixed after 1h of

121 incubation at room temperature dried, and resuspended in 2% acetonitrile (AcN), 0.1% TFA
122 (Sigma-Aldrich).

123 *iTRAQ sample analysis*

124 Samples were analyzed per UPLC-TandemMS in technical duplicates. Labeled peptides were
125 separated by a nanoUPLC system (Thermo Scientific, USA) coupled online to a Q Exactive HF MS
126 (Thermo Scientific) using a reverse phase C18 trapping column setup with 75cm main column
127 (Thermo Scientific) with loading in 2% solvent B (0.1% FA in AcN) gradient and separated by
128 176min gradient from 11%B to 30%B with a constant flow rate at 250nL/min. MS was operated in
129 positive mode using Top10 data-dependent acquisition (MS1 m/z 375-1,500 at R 120,000) and
130 tandems sequencing using fixed m/z range at 110 and a MS2 resolution of 15,000.

131 *Database searches*

132 Raw data were processed using Proteome Discoverer v2.3.0.523 (Thermo Scientific). Sequest HT
133 was set as the search engine against the reviewed Uniprot Homo sapiens reference protein database
134 (09/2017). iTRAQ 4-plex labeling of N-terminal and lysine and carbamidomethylation (C) were set
135 as fixed modifications while oxidation (M), deamidation (N/Q) and protein N-terminal acetylation
136 were included as variable modifications. Precursor mass tolerance and fragment mass tolerance
137 were set at 10ppm and 0.05Da, respectively. PSMs were filtered using percolator with a strict false
138 discovery rate (FDR) of 1% and a relaxed FDR of 5%. Unique and razor peptides were used for
139 quantification, and iTRAQ channels were normalized to total peptide amount. Master proteins were
140 filtered for high protein FDR confidence. MS data have been deposited to the ProteomeXchange
141 Consortium via the PRIDE [39] partner repository with the dataset identifier PXD014037.

142 *Bioinformatics analyses and functional annotation of regulated proteins*

143 Normalized abundances were used for further analyses of proteins identified with two or more
144 unique peptides. Data distribution was assessed with Perseus v.1.5.3.2 software and differentially

regulated features were selected using t-test with a post-hoc background-based adjusted p-value<0.05 [35]. Venny 2.1 (http://bioinfogp.cnb.csic.es/tools/venny) was used to compare the regulated proteins among the different comparisons. ToppGene Suite[8] was used for functional enrichment of regulated proteins according to Gene Ontology (GO) terms and pathway analysis. Enriched lists were further accessed by String app on Cytoscape v3.6.1 [44].

Reverse transcription quantitative PCR (RT-qPCR) analysis of *FOXP3, MYOG,* and *MMP13* in SS and deltoid muscle tissue

RNA extraction

Muscle biopsies (n=18/group) were isolated using TRIzol® Reagent. Phase separation was performed using chloroform and isopropyl alcohol was used to precipitate RNA. The RNA concentrations and purities were determined using a Nanodrop Spectrophotometer (Thermo Scientific).

cDNA synthesis

RNA samples were diluted to obtain a concentration of 250ng/µL, and reverse transcription was performed using an Applied Biosystem kit according to the manufacturer's instructions. The synthesis was performed using an MJ Research PTC-225 Gradient Thermal Cycler (Marshall Scientific). cDNA samples were diluted to lower the concentrations to ~50ng/μL.

RT-qPCR

RT-qPCR was performed using a CFX Connect Real-Time PCR Detection System (Bio-Rad) and analyzed using SYBR green. Samples were run against standard curves generated from serial dilutions from a pool of all samples. Values were normalized to *ACTB* (β-actin) as the reference gene and calibrated to a pool of cDNA obtained from one pectoralis and one subscapularis muscle biopsy. Triplicates of all samples, standards, and negative controls were conducted. To ensure no

sign of primer dimer formation or contamination, a no amplification control (NAC), a no template control (NTC), and a no reverse transcriptase (NRT) were included as controls.

RT-qPCR cycling conditions were as follows: 10min at 95℃, followed by 40 cycles of denaturing at 95℃ for 15 seconds, 30 seconds at annealing temperature, and extension at 72℃ at 30 seconds. Primer sequences were: *ACTB*, sense 5´-GGCCACGGCTGCTTC-3´ and anti-sense 5´-GTTGGCGTACAGGTCTTTGC-3´ (T_a 52℃ and T_m 84℃), *FOXP3*, sense 5´-CCCGGATGTGAGAAGGTCTT-3´ and anti-sense 5´-TTCTCCTTCTCCAGCACCAG-3´ (T_a 57℃ and T_m 82℃), *MYOG*, sense 5´-GCCCTGATGCTAGGAAGCC–3´ and anti-sense 5´-CTGAATGAGGGCGTCCAGTC-3´ (T_a 70℃ and T_m 85℃), and *MMP13*, sense 5´-CGC CAG ACA AAT GTG ACC CT-3´ and anti-sense 5´-CAG GCG CCA GAA GAA TCT GT-3´ (T_a 55℃ and T_m 77℃). Primer specificity was ensured by generation and evaluation of melting curves. Primers were purchased from TAG Copenhagen.

Electrochemiluminescence analysis

Protein purification

Tendon and muscle samples were homogenized at 4°C in Mesoscale Lysis buffer containing Phosphatase Inhibitor Cocktail 2 and 3 (Sigma-Aldrich) and Complete Mini EDTA-free Protease Inhibitor (Roche). Protein content was measured by the bicinchoninic acid method using the Thermo Scientific Micro BCA™ Protein assay Kit (Pierce Chemical Co) [40].

Multiplex analysis

Protein concentrations in tendon and muscle samples were measured using an MSD human U-Plex Biomarker Multip-Plex Kit, a U-PLEX human TGF-β Combo Kit, a human MMP 3-Plex Ultra-Sensitive Kit, and human TNF-RI and TNF-RII Ultra-Sensitive Kits (all from Mesoscale), using the MSD QuickPlex (SQ120) Plate Reader (Mesoscale) according to the manufacturer's instructions.

ICAM-1 and VCAM-1 analyses were performed on SS and deltoid muscle tissue using V-PLEX Vascular Injury Panel 2 (Mesoscale). Samples were run in duplex and diluted 2- or 4-fold in Diluent 41 prior to measurement. Data were analyzed using MSD Discovery Workbench software. The lower limit of detection was a calculated concentration based on a signal 2.5 standard deviations (SD) above the blank (zero) calibrator and coefficient of variation (CV) values below 25% were accepted.

Statistical analysis

To examine differences in protein expression between SS and deltoid muscle tissue, paired Student's t-test was used. Correlation analyses between cytokine, MMPs, and growth factors versus age of lesion used Spearman's test.To examine the correlation between the relative expression of *FOXP3*, *MYOG*, and *MMP13* in SS and deltoid muscles, a paired Wilcoxon test was carried out. The outlier test ROUT was used to identify and remove outliers more than 2 SD from the dataset. All statistical analyses were carried out using GraphPad Prism. P-values ≤ 0.05 were considered statistically significant. Data are presented as mean±SD or median (25, 75 interquartile range, IQR).

Results

Mass spectrometry-based proteomics analysis shows protein regulation upon RC lesion

Using quantitative mass spectrometry (MS) proteomics, a total of 2,463 proteins were identified, of which 1,895 had two or more unique peptides (Supplementary Table S2). Moreover, 417 quantified proteins were shared by all tissues of all patients and could be assessed by principal component analysis (PCA) (Supplementary Figure 1A), which showed a clear distribution pattern even in the absence of well-delimited clusters.

To better understand protein regulation underlying RC pathology, SS muscle protein expression pattern was compared to deltoid as a non-RC shoulder muscle control. A total of 239 proteins were regulated. Of these, 114 were more highly expressed in the SS muscle (Figure 2A, Supplementary Table S3). Gene ontology analysis showed 'extracellular matrix organization' and 'neutrophil degranulation' among the most enriched biological processes (Supplemental Figure 2, Table S4) while 'degradation of extracellular matrix', 'innate immune system' and 'neutrophil degranulation' were among the enriched pathways of upregulated proteins (Figure 2B, Supplementary Figure 2, and Supplementary Table S4). Interestingly, 'mitochondrial cellular localization', and 'muscle system process' were among the enriched annotations of downregulated proteins (Figure 2B, Supplementary Figure 3, and Table S4). A detailed list of regulated proteins involved in the above-mentioned processes, along with experimental ratio, are provided in Figure 2C-K.

To address the molecular response of different RC tissues, the comparison between SS muscle and SS tendon showed 139 differentially expressed proteins (Supplementary Table S5). Pathways or gene ontologies related to immune response or inflammatory processes were not enriched among these regulated proteins.

In contrast, pointing towards a common molecular signature between SS muscle and SS tendon in RC disease, 38 proteins were regulated in both tissues when compared to deltoid muscle (Supplementary Figure 1B, Supplementary Tables S6 and S7). Several of these proteins were related to catalytic activity, with mitochondrial protein complex being the main cellular component (Supplementary Figure 1C).

RC lesion results in atrophy and lipid accumulation

Staining with hematoxylin & eosin revealed muscle fiber changes already 1½ months after tendon lesion represented by internalization of nuclei and muscle fibers of varying size after the tendon tear

(Figure 3A). In addition, pathological infiltrating adipocytes were detected, as substantial fat infiltration was seen together with arrays of intracellular myonuclei and varying fiber size, suggestive of degeneration (Figure 3B,C).

Inflammatory changes appeared to be intensified from 1½ months to 6 months with abundant stromal inflammatory phagocytic cells represented by the presence of $CD68^+$ macrophages (Figure 3D and 3E). At 24 months, degeneration was clearly seen with a substantial proportion of muscle cells replaced by fat cells indicative of muscle cell degeneration (Figure 3F). At 24 months, absent or few $CD68^+$ positive cells indicated decreased inflammation. The deltoid muscle did not demonstrate similar inflammatory and degenerative changes (Figure 3G-L).

Adipophilin/perilipin-2 immunohistochemistry for detection of lipids in myofibers demonstrated that adipophilin was localized to the surface of intra-cellular lipid droplets (Figure 4). The expression varied both between patients (please compare Figure 4A and Figure 4C) and between muscles from the same patient (please compare Figure 4A with Figure 4B). Regional differences within muscles were also seen (Figure 4), and some individual fibers presented increased lipid accumulation both as number and size of droplets.

RC tendon tear leads to changes in inflammatory mediators in SS muscle

None of the patients showed any signs of peripheral inflammation as mean blood leukocyte counts, hemoglobin, and C-reactive protein values were within normal ranges and all patients were negative for rheumatic factors. Given the findings of significant changes in the proteome of SS compared to deltoid muscle after RC tear, we investigated changes in a variety of pro- and anti-inflammatory cytokines, chemokines, receptors, and growth factors (Figure 5 and Table 1). We found lower CCL19 levels (Figure 5A) but higher CXCL5 levels (Figure 5B) in the SS compared to the deltoid muscle. IL-1β (Figure 5C), IL-6 (Figure 5D), IL-8 (Figure 5E), and IL-33 levels (Figure 5F) were

higher in SS compared to deltoid muscle. IL-7 levels (Figure 5G), IL-15 (Figure 5H), IL-17A (Figure 5I), and IFN-α2a levels (Figure 5J) were in SS compared to deltoid muscle. Despite comparable levels of TNF (Figure 5K), TNFR1 (Figure 5L) and TNFR2 (Figure 5M) levels were changed in the SS muscle compared to the deltoid after RC tendon tear. G-CSF levels were lower in SS muscle compared to the deltoid (Figure 5N).

We observed no significant correlation between age of lesion and CCL19 (r=-0.05, p=1), CXCL5 (r=-0.26, p=0.31) , IL-1β (r=-0.30, p=0.3) , IL-6 (r=-0.48, p=0.07) ,IL-8 (r=-0.43, p=0.11) , IL-33 (r=0.16, p=0.54) , IL-7 (r=0.35, p=0.39), IL-15 (r=0.07, p=0.79), IL-17A (r=0.09, p=0.76), IFN-α2a (r=0.39, p=0.3), TNF (r=-0.39, p=0.15) , TNFR1 (r=-0.4, p=0.29), TNFR2 (r=-0.16, p=0.66), or G-CSF (r=0.16, p=0.71).

Finally, several cytokine levels were similar in SS and deltoid muscle (Table 1). The concentration of most cytokines, chemokines, growth factors, and MMPs was high in the SS tendon (Supplementary Table 8).

The regenerative potential appears to be impaired in the SS muscle after RC tendon tear

IL-17 production characterizes pro-inflammatory T helper 17 lymphocytes (Th17) and innate immune cells [11]. Th17 has been shown to have opposing effects in the immune response from regulatory T cells (Treg) [49], which is important in muscle regeneration (reviewed in [7]) and whose master gene is the transcription factor Forkhead box P3 (FOXP3). We found decreased IL-17A levels in SS muscle compared to deltoid muscle (Figure 5G). Therefore, we next investigated *FOXP3* mRNA expression and found that *FOXP3* mRNA levels were significantly lower in SS muscle compared to deltoid muscle (Figure 6A). However, when we counted $FOXP3^+$ cells (Figure 6B) and $CD3^+$ T cells (Figure 6C) in SS and deltoid muscle tissue sections (Figure 6D), we did not observe any significant differences in the number of $FOXP3^+$ cells/mm^2 or $CD3^+$ T cells/mm^2.

289 Approximately 7.5% of all T cells in the SS muscle were FOXP3^{+} Treg cells (overlay in Figure 6D,
290 upper panel), and approximately 13% of all T cells in the deltoid muscle were FOXP3^{+} Treg cells
291 (overlay in Figure 6D, middle panel). The number of T cells/mm^{2} were, however, quite variable
292 (Figure 6D).
293 To investigate gene expression levels involved in myogenesis, we estimated *MYOG* expression and
294 found the relative mRNA levels to be significantly decreased in the SS compared to the deltoid
295 muscle (Figure 6E).
296
297 **Changes in matrix metalloproteinases and transforming growth factors after RC tendon tear**
298 As gene ontology analysis showed changes in proteins involved in 'extracellular matrix
299 organization', we investigated changes in the levels of 4 matrix metalloproteinases (MMPs) known
300 to be involved in the degradation of the extracellular matrix [38].
301 We did not observe any differences in MMP1 levels between SS and deltoid muscle (Figure 7A).
302 However, levels of MMP3 (that is known to degrade collagen types II-IV, IX, and X and to have
303 important regulatory functions such as activation of other MMPs) were significantly higher in SS
304 compared to deltoid muscle (Figure 7B). Furthermore, levels of MMP-9 (known to degrade
305 collagen fragments IV and V) were changed (Figure 7C) suggesting decreased MMP-9 levels in
306 deltoid compared to SS muscle.
307 *MMP13* (known to degrade primarily collagen fragments II) mRNA gene expression was absent in
308 SS (0.005 ± 0.006, n=12) and deltoid (0.002 ± 0.002, n=16) muscle tissue, whereas *MMP13* mRNA
309 gene expression was present in SS tendon tissue (4.95 ± 5.33, n=4) in RC tear conditions.
310 A significant negative correlation was found between age of lesion and MMP9 levels (r=-0.61,
311 p=0.03). We found no significant correlation between age of lesion and MMP1 levels (r=0.05,
312 p=0.87) and a tendency of a correlation with MMP3 levels ((r=-0.46, p=0.08).

In line with previous findings in the SS enthesis (reviewed in [22]), we found that protein levels of MMP-1 (known to specifically break down most subtypes of collagen, providing mechanical strength to tissues) were higher in SS tendon than in muscle tissue (Supplementary Table 8). Also, MMP-3 was high in the SS tendon (Supplementary Table 8).

We also investigated changes in transforming growth factors (TGF), known to be affected in SS enthesis following RC tear (reviewed in [22]) (Figure 7D-F). Levels of TGFβ1 (Figure 7D) and TGFβ3 (Figure 7F) were higher in SS muscle, suggesting increased TGFβ1 and TGFβ3 levels in SS muscle compared to deltoid muscle. We found no correlation between age of lesion and TGFβ1 ($r=0.12$, $p=0.7$), TGFβ2 ($r=-0.07$, $p=0.83$), or TGFβ3 ($r=-0.32$, $p=0.34$).

Discussion

In this study, we demonstrated massive SS muscle inflammation after tendon tear combined with fatty infiltration and degeneration. Simultaneous changes in the innate immune response, cytokines, and proteins related to extracellular matrix reorganization and mediation of fibrosis in the SS musculature were also seen.

In line with previous experimental studies using mice [28] and rats [12; 17; 18] we observed high numbers of infiltrating monocytes/macrophages in SS muscle in early cases of tendon tear; this tendency ceased after 24 months, however. Inflammation was (initially) driven by high numbers of infiltrating $CD68^+$ macrophages, which are thought to be key sources of TGF-β1 linked to fibrosis in chronically injured muscle [30].

Upregulated proteins in SS muscle compared to deltoid also showed ‘neutrophil degranulation’ among the most enriched processes. Neutrophils have been identified as the main cells infiltrating the muscle after injury [46], and neutrophil-derived oxidants extended tissue damage in a rabbit model of stretch skeletal muscle injury [47]. On the other hand, blocking cell infiltration compromised the initial regenerative response, suggesting a role for neutrophils in muscle growth and repair by

removal of tissue debris and activation of satellite cells [47]. Moreover, a recent study has shown that neutrophil-secreted proteases can also have an immunoregulatory role by activating IL-33 [9]. IL-33 has been shown to be produced by fibro-adipogenic progenitor (FAP) cells, which are uniformly present in the interstitial space in skeletal muscle and respond to muscle damage [20]. Our observation of higher IL-33 levels in SS muscle compared to deltoid muscle indicate an activation of FAPs, which are the source of adipocytes in muscle fatty infiltration. Muscle $Foxp3^+$ regulatory T cells (Tregs) are characterized by high levels of expression of the IL-33 receptor, ST2, and are known to potentiate regeneration in acute and chronic injury models [7]. Despite comparable numbers of $Foxp3^+$ Tregs/mm^2, we saw a significant decrease in *FOXP3* mRNA levels in SS muscle compared to deltoid muscle following RC tear, suggestive of repressed gene expression in Tregs located in SS muscle. Many cytokines and factors can negatively regulate *FOXP3* gene expression, including IL-6, IL-7, TGF-β, and G-CSF, [21; 32; 42], all of which we observed to be different between SS and deltoid muscle.

The expression of IL-15 has been shown to inhibit fatty infiltration and facilitate muscle regeneration through regulation of FAP cells [23]. In the present study, IL-15 levels were significantly lower in the SS compared to the deltoid muscle, supporting our findings that adipocytes appear in the SS and that the regenerative potential appears to be reduced in SS muscle after RC tendon tear.

IL-17 is a pro-inflammatory cytokine secreted by activated $CD4^+$ T-helper cells (Th17), which are highly pro-inflammatory and induce severe autoimmunity (reviewed in [27]). IL-17 levels are increased in early human tendinopathy, mediating inflammatory and tissue remodeling events [34], and IL-17 inhibits myoblast differentiation [26]. In the present study, IL-17 levels were significantly lower in SS than in deltoid muscle, but the exact relevance of decreased IL-17 levels remains to be elucidated.

Our gene ontology analysis showed changes in 'extracellular matrix organization' and 'degradation of extracellular matrix' especially due to the upregulation of CMA1, COL5A3, CTSS, ELN, and MMP19 in SS compared to deltoid muscle. To our knowledge, no one has investigated MMP levels in human SS muscle under tear conditions. MMPs are a large group or proteolytic enzymes responsible for tissue remodeling and degradation of extracellular matrix. In our study, MMP-3 and MMP-9 levels were significantly increased in SS compared to deltoid muscle. MMP-3 is one of the primary activators of MMP-9 from its inactive proenzyme form [36]. MMP-9 is produced by a variety of cells, including fibroblasts. MMP-9 appears to be a regulatory factor in neutrophil migration across the basement membrane [13], and it also plays several important functions within neutrophil action [27] such as degrading extracellular matrix, activation of IL-1β, and cleavage of several chemokines [37]. In vitro studies have demonstrated that inhibition of MMP-9 reduced the levels of active TGF-β1 and reduced several TGF-β1-driven responses such as fibroblast stimulation [25]. In this context, MMP-9 appears to activate or stimulate the release of a number of cytokines and growth factors, including TGF-β1 [31], which we found to be elevated in SS compared to deltoid muscle. MMP-9 activity positively correlated to skeletal muscle atrophy in immobilized rats [41], supporting a role in muscle atrophy. This is in line with our present findings of a positive correlation between MMP-9 levels and age of RC lesion. Altogether, this suggests that MMP-9 plays an important role in SS muscle remodeling.

While only a few studies have applied a large-scale proteomics approach to address RC pathophysiology, these studies combined found several markers indicative of tissue remodeling and suggested an untapped potential for proteomics in tendon research (reviewed in [43]). A multi-omics methodology applied to a rat RC injury model to study myosteatosis identified disrupted mitochondrial function as one of the underlying mechanisms of lipid accumulation in muscle fibers [19]. In our study, we identified 32 downregulated mitochondrial proteins, 15 of which are associated

with mitochondrial electron transport chain. Mitochondrial dysfunction reduces energy production and the dysfunction of these organelles has been connected to the myosteatosis that is commonly reported following RC tendon injury [3]. Our finding of steatotic adipophilin positive muscle fibers and changes in lipid metabolism and mitochondrial function supports this connection.

This study has certain inherent limitations related to the variability of disease severity and duration and the sample size, and the results are biased towards patients with RC tears who chose to undergo surgery. The enrolled patients comprised four smokers and seven patients who received pain killers on a daily basis. The adverse consequences of smoking and mild anti-inflammatory drug intake on the inflammatory response was not assessed due to lack of statistical power. Another limitation inherent in muscle biopsy studies is the difficulty of ensuring uniform biopsy procedures, which are important to secure reproducibility and to account for regional variations in protein composition. In this study, biopsies were obtained close to the musculotendinous junction of the SS muscle in all patients using an all-arthroscopic approach from the bursal side, limiting possible location-dependent variations.

The rationale for using the deltoid muscle for comparison could be challenged as it may be asymptomatically affected. The ipsilateral deltoid has been used as a standard of reference in a number of studies [2; 13], also justifying the use of paired statistics and increasing the power of the analyses.

Conclusions

This study demonstrated massive muscle changes after SS tendon tear characterized by high numbers of inflammatory macrophages in lesions less than three months old and overall changes in cytokine levels, MMP levels, and growth factors. Our proteome analysis demonstrated that proteins

involved in inflammation, extracellular matrix reorganization, and lipid metabolism were among the most enriched. Knowing that massive inflammation with infiltration of immune cells into the RC musculotendinous lesion disrupt normal muscle regeneration, this implies that intervention with repair of the tendon lesion and concomitant target-specific adjuvant treatment of the inflammatory state of the SS muscle could be key to improving RC muscle recovery.

Figure legends

Figure 1. Schematic workflow applied to the study of molecular pathways involved in the RC lesion. Biopsies of supraspinatus tendon and supraspinatus and deltoid muscle biopsies from ten patients undergoing surgery for partial or full-thickness RC were evaluated.

Figure 2. Proteomics of muscle biopsies. (A) Differentially regulated protein pattern between SS and deltoid muscles from patients with RC lesion (FDR 5%). Downregulated proteins are represented in blue and upregulated in red. Dotted lines highlight proteins at least 2 times overrepresented in each tissue. (B) Protein-protein network of SS vs deltoid muscle-regulated proteins grouped according functional enrichment. Underrepresented proteins in SS muscle are shown in blue while overrepresented are shown in red. (C-K) Levels of upregulated (red) or downregulated (blue) proteins involved in Leukocyte mediated immunity (C), Immune effector process (D), Immune system (E), Positive regulation of lipid metabolic processes (F), Metabolism of lipids (G), Electron transport chain (H), Muscle structure development (J), Extracellular matrix organization (I), and Striated muscle contraction (K) as measured by proteomics (n=10 muscles per group). Abbreviations: ADAR, double-stranded RNA-specific adenosine deaminase; ADIPOQ, adiponectin; ALDH5A1, succinate-semialdehyde dehydrogenase, mitochondrial; ANKRD1, ankyrin repeat domain-containing protein 1; ANKRD2, ankyrin repeat domain-containing protein 2; AP1B1, AP-complex subunit beta-1; APOA1, apolipoprotein A-1; APOA2, apolipoprotein A-2; APOA4, apolipoprotein A-4; APOE, apolipoprotein E; CMA1, chymase; COL5A3, collagen alpha-3(V) chain; COX6A1, cytochrome c oxidase subunit 6A1; COX6A2, cytochrome c oxidase subunit 6A2; COX6B1, cytochrome c oxidase subunit 6B1; CTSA, cathepsin A; CTSC, cathepsin C; CTSS, cathepsin S; DNM1, dynamin-1; DNM2, dynamin-2; EEF1A2, elongation factor-1 alpha; ELN,

elastin; ENG, endoglin; F2, prothrombin; FABP4, fatty acid-binding protin; FASN, fatty acid synthase; FBN1, fibrillin-1; FDXR, NADPH:adrenodoxin oxidoreductase, mitochondrial; FITM2, fat storage-inducing transmembrane protein 2; GGH, gamma-glutamyl hydrolase; GLRX5, glutaredoxin-related protein 5, mitochondrial; GNS, N-acetylglucosamine-6-sulfatase; GSR, glutathione reductase, mitochondrial; HEXA, beta-hexosaminidase subunit alpha; HLA-A, HLA class I histocompatibility antigen, A-31 alpha chain; HPGDS, hematopoietic prostaglandin D synthase; HUWE1, E3 ubiquitin-protein ligase; ICAM1, intercellular adhesion molecule 2; LGALS1, galectin-1; MFAP4, microfibril-associated glycoprotein 4; MMP19, matrix metalloproteinase-19; MYH3, myosin-3; MYH7, myosin-7; MYL2, myosin light chain 2; MYL3, myosin light chain 3; MYL6B, myosin light chain 6B; MYOZ2, myozenin-2; ND4, NADH-ubiquinone oxidoreductase chain 4; NDUFA4, cytochrome c oxidase subunit NDFUA4; NDUFA9, NADH dehydrogenase [ubiquinone] 1 alpha subcomplex subunit 9, mitochondrial; NDUFAB1, acyl carrier protein, mitochondrial; NDUFB3, NADH dehydrogenase [ubiquinone] 1 beta subcomplex subunit 3; NDUFC2, NADH dehydrogenase [ubiquinone] 1 subunit C2; NDUFS5, NADH dehydrogenase [ubiquinone] iron-sulfur protein 5; NDUFS7, NADH dehydrogenase [ubiquinone] iron-sulfur protein 7, mitochondrial; NUP62, nuclear pore glycoprotein p62; OSTF1, osteoclast-stimulating factor 1; PLIN1, perilipin-1; PON2, serum paraoxonase/arylesterase 2; PPT1, palmitoyl-protein thioesterase 1; PRDX4, peroxiredoxin-4; PTPRC, receptor-type tyrosine-protein phosphatase C; PYCARD, apoptosis-associated speck-like protein containing a CARD; SACM1L, phosphatidylinositide phosphatase SAC1; SERPINB12, serpin B12; SLC25A1, tricarboxylate transport protein, mitochondrial; SNRPA1, U2 small nuclear ribonucleoprotein A; SORBS1, sorbin and SH3 domain-containing protein 1; TNNI1, troponin I, slow skeletal muscle; TNNT1, troponin T, slow skeletal muscle; UCHL1, ubiquitinin carboxyl-terminal hydrolase isozyme L1; UQCR11, cytochrome b-c1 complex subunit 10; VCAM1, vascular cell adhesion protein 1.

Figure 3. Histological analysis of SS muscle. (A-C) H&E-stained tissue sections of SS muscle biopsies from representative patients at 1½ months (A), 6 months (B), and 28 months (C) after RC tendon tear demonstrating the presence of muscle fibers with internal nuclei (arrows) and nuclear chains (arrow heads). (D-F) Immunohistochemical staining of SS muscle biopsies from representative patients at 2½ months (D), 6 months (E), and 28 months (F) demonstrating the presence of a high number of $CD68^+$ macrophages (arrows) within the first 6 months after RC tendon tear. Please note the presence of massive fatty cell infiltration (*, asterisks) between muscle

fibers already early after RC tendon tear. (G-I) H&E-stained tissue sections of deltoid biopsies from representative patients at 1½ months (G), 6 months (H), and 24 months (I) after RC tendon tear. (J-L) CD68 immunohistochemical staining of deltoid muscle biopsies biopsies from representative patients at 1½ months (J), 6 months (K), and 24 months (L) after RC tendon tear. Scale bar: 100µm.

Figure 4. Immunohistochemical staining for adipophilin. (A,B) Adipophilin expression in SS (A) and deltoid (B) muscle fibers in a patient with a 6-month-old RC lesion, showing higher adipophilin expression in the SS muscle compared to the deltoid. Adipophilin is seen as a granular staining in the muscle fiber cytoplasm and due to its localization to the surface of lipid vacuoles, it visualizes the distribution one of intracellular lipid. (C,D) Adipophilin expression in SS and deltoid muscle fibers from patient with a >72-month-old RC tear (C) and another patient with a 7-month-old RC lesion (D). Please note that the distribution of adipophilin can be uneven with different expression in neighboring fascicles in both the SS and deltoid muscles. Scale bar: 100µm.

Figure 5. Cytokine and TNF receptor protein expression in SS and deltoid muscle tissue in RC tear conditions. (A-N) Electrochemiluminescence immunoassay analysis of CCL19 (A), CXCL5 (B), IL-1β (C), IL-6 (D), IL-8 (E), IL-33 (F), IL-7 (G), IL-15 (H), IL-17A (I), INF-α2a (J), TNF (K), TNFR1 (L), TNFR2 (M), and G-CSG (N) protein levels in SS and deltoid muscle biopsies from patients with RC tendon tear. ***p<0.001, **p<0.01. *p<0.05, Student's t-test (n = 22/group). Samples with CV values above 25% were excluded in individual analyses.

Figure 6. *FOXP3* and *MYOG* mRNA expression is lower in SS muscle than in deltoid muscle tissue in RC tear conditions. (A) *FOXP3* mRNA levels in SS and deltoid muscle biopsies demonstrated significantly lower expression levels in SS compared to deltoid muscle. **p<0.01, paired Student's t-test (n=18/group). Two outliers in the SS muscle and two outliers in the deltoid muscle group were removed according to ROUT's outlier test. (B-C) The number of $FOXP3^+$ Treg cells/mm^2 (B) and the total number of $CD3^+$ T cells (C) were comparable between SS and deltoid muscle in RC tear conditions. (D) Representative FOXP3 and CD3 immunohistochemically stained tissue sections from SS and deltoid muscle demonstrating overlay between subsets of $FOXP3^+$ and $CD3^+$ T cells, representing the presence of Treg cells (arrows) in both SS and deltoid muscle in RC tear conditions. Scale bars: 50µm (top and middle panels) and 100µm (bottom panel). (E) *MYOG*

mRNA levels in SS and deltoid muscle biopsies demonstrated significantly lower expression levels in SS compared to deltoid muscle. **p<0.01, paired Student's t-test (n=18/group).

Figure 7. Matrix metalloprotease and transforming growth factor-β protein expression in SS and deltoid muscle tissue under RC tear conditions. (A-F) Electrochemiluminescence immunoassay analysis of MMP-1 (A), MMP-3 (B), MMP-9 (C), TGFβ1 (D), TGFβ2 (E), and TGFβ3 (F) protein levels in SS and deltoid muscle biopsies from patients with RC tendon tear. *p<0.05, Student's test (n = 22/group). Samples with CV values above 25% were excluded in individual analyses.

References

1. Abrams GD, Luria A, Carr RA, Rhodes C, Robinson WH, Sokolove J. Association of synovial inflammation and inflammatory mediators with glenohumeral rotator cuff pathology. J Shoulder Elbow Surg 2016;25:989-997. 10.1016/j.jse.2015.10.011
2. Ashry R, Schweitzer ME, Cunningham P, Cohen J, Babb J, Cantos A. Muscle atrophy as a consequence of rotator cuff tears: should we compare the muscles of the rotator cuff with those of the deltoid? Skeletal Radiol 2007;36:841-845. 10.1007/s00256-007-0307-5
3. Bedi A, Dines J, Warren RF, Dines DM. Massive tears of the rotator cuff. J Bone Joint Surg Am 2010;92:1894-1908. 10.2106/JBJS.I.01531
4. Bennike TB, Carlsen TG, Ellingsen T, Bonderup OK, Glerup H, Bogsted M et al. Neutrophil Extracellular Traps in Ulcerative Colitis: A Proteome Analysis of Intestinal Biopsies. Inflamm Bowel Dis 2015;21:2052-2067. 10.1097/MIB.0000000000000460
5. Benson RT, McDonnell SM, Knowles HJ, Rees JL, Carr AJ, Hulley PA. Tendinopathy and tears of the rotator cuff are associated with hypoxia and apoptosis. J Bone Joint Surg Br 2010;92:448-453. 10.1302/0301-620X.92B3.23074
6. Blaine TA, Kim YS, Voloshin I, Chen D, Murakami K, Chang SS et al. The molecular pathophysiology of subacromial bursitis in rotator cuff disease. J Shoulder Elbow Surg 2005;14:84S-89S. 10.1016/j.jse.2004.09.022
7. Burzyn D, Kuswanto W, Kolodin D, Shadrach JL, Cerletti M, Jang Y et al. A special population of regulatory T cells potentiates muscle repair. Cell 2013;155:1282-1295. 10.1016/j.cell.2013.10.054

8. Chen J, Bardes EE, Aronow BJ, Jegga AG. ToppGene Suite for gene list enrichment analysis and candidate gene prioritization. Nucleic Acids Res 2009;37:W305-311. 10.1093/nar/gkp427
9. Clancy DM, Sullivan GP, Moran HBT, Henry CM, Reeves EP, McElvaney NG et al. Extracellular Neutrophil Proteases Are Efficient Regulators of IL-1, IL-33, and IL-36 Cytokine Activity but Poor Effectors of Microbial Killing. Cell Rep 2018;22:2937-2950. 10.1016/j.celrep.2018.02.062
10. Cofield RH, Parvizi J, Hoffmeyer PJ, Lanzer WL, Ilstrup DM, Rowland CM. Surgical repair of chronic rotator cuff tears. A prospective long-term study. J Bone Joint Surg Am 2001;83:71-77.
11. Cua DJ, Tato CM. Innate IL-17-producing cells: the sentinels of the immune system. Nat Rev Immunol 2010;10:479-489. 10.1038/nri2800
12. Davies MR, Lee L, Feeley BT, Kim HT, Liu X. Lysophosphatidic acid-induced RhoA signaling and prolonged macrophage infiltration worsens fibrosis and fatty infiltration following rotator cuff tears. J Orthop Res 2017;35:1539-1547. 10.1002/jor.23384
13. de Witte PB, Werner S, ter Braak LM, Veeger HE, Nelissen RG, de Groot JH. The Supraspinatus and the Deltoid - not just two arm elevators. Hum Mov Sci 2014;33:273-283. 10.1016/j.humov.2013.08.010
14. Gibbons MC, Singh A, Anakwenze O, Cheng T, Pomerantz M, Schenk S et al. Histological Evidence of Muscle Degeneration in Advanced Human Rotator Cuff Disease. J Bone Joint Surg Am 2017;99:190-199. 10.2106/JBJS.16.00335
15. Gladstone JN, Bishop JY, Lo IK, Flatow EL. Fatty infiltration and atrophy of the rotator cuff do not improve after rotator cuff repair and correlate with poor functional outcome. Am J Sports Med 2007;35:719-728. 10.1177/0363546506297539
16. Gumucio J, Flood M, Harning J, Phan A, Roche S, Lynch E et al. T lymphocytes are not required for the development of fatty degeneration after rotator cuff tear. Bone Joint Res 2014;3:262-272. 10.1302/2046-3758.39.2000294
17. Gumucio JP, Davis ME, Bradley JR, Stafford PL, Schiffman CJ, Lynch EB et al. Rotator cuff tear reduces muscle fiber specific force production and induces macrophage accumulation and autophagy. J Orthop Res 2012;30:1963-1970. 10.1002/jor.22168

18. Gumucio JP, Korn MA, Saripalli AL, Flood MD, Phan AC, Roche SM et al. Aging-associated exacerbation in fatty degeneration and infiltration after rotator cuff tear. J Shoulder Elbow Surg 2014;23:99-108. 10.1016/j.jse.2013.04.011
19. Gumucio JP, Qasawa AH, Ferrara PJ, Malik AN, Funai K, McDonagh B et al. Reduced mitochondrial lipid oxidation leads to fat accumulation in myosteatosis. FASEB J 2019;33:7863-7881. 10.1096/fj.201802457RR
20. Hejbol EK, Hajjaj MA, Nielsen O, Schroder HD. Marker Expression of Interstitial Cells in Human Skeletal Muscle: An Immunohistochemical Study. J Histochem Cytochem 2019;67:825-844. 10.1369/0022155419871033
21. Heninger AK, Theil A, Wilhelm C, Petzold C, Huebel N, Kretschmer K et al. IL-7 abrogates suppressive activity of human CD4+CD25+FOXP3+ regulatory T cells and allows expansion of alloreactive and autoreactive T cells. J Immunol 2012;189:5649-5658. 10.4049/jimmunol.1201286
22. Jensen PT, Lambertsen KL, Frich LH. Assembly, maturation, and degradation of the supraspinatus enthesis. J Shoulder Elbow Surg 2018. 10.1016/j.jse.2017.10.030
23. Kang X, Yang MY, Shi YX, Xie MM, Zhu M, Zheng XL et al. Interleukin-15 facilitates muscle regeneration through modulation of fibro/adipogenic progenitors. Cell Commun Signal 2018;16:42. 10.1186/s12964-018-0251-0
24. Karjalainen TV, Jain NB, Heikkinen J, Johnston RV, Page CM, Buchbinder R. Surgery for rotator cuff tears. Cochrane Database Syst Rev 2019;12:CD013502. 10.1002/14651858.CD013502
25. Kobayashi T, Kim H, Liu X, Sugiura H, Kohyama T, Fang Q et al. Matrix metalloproteinase-9 activates TGF-beta and stimulates fibroblast contraction of collagen gels. American journal of physiology Lung cellular and molecular physiology 2014;306:L1006-1015. 10.1152/ajplung.00015.2014
26. Kocic J, Santibanez JF, Krstic A, Mojsilovic S, Ilic V, Bugarski D. Interleukin-17 modulates myoblast cell migration by inhibiting urokinase type plasminogen activator expression through p38 mitogen-activated protein kinase. Int J Biochem Cell Biol 2013;45:464-475. 10.1016/j.biocel.2012.11.010
27. Kotake S, Yago T, Kawamoto M, Nanke Y. Role of osteoclasts and interleukin-17 in the pathogenesis of rheumatoid arthritis: crucial 'human osteoclastology'. J Bone Miner Metab 2012;30:125-135. 10.1007/s00774-011-0321-5

28. Krieger JR, Tellier LE, Ollukaren MT, Temenoff JS, Botchwey EA. Quantitative analysis of immune cell subset infiltration of supraspinatus muscle after severe rotator cuff injury. Regen Eng Transl Med 2017;3:82-93. 10.1007/s40883-017-0030-2
29. Kuenzler MB, Nuss K, Karol A, Schar MO, Hottiger M, Raniga S et al. Neer Award 2016: reduced muscle degeneration and decreased fatty infiltration after rotator cuff tear in a poly(ADP-ribose) polymerase 1 (PARP-1) knock-out mouse model. J Shoulder Elbow Surg 2017;26:733-744. 10.1016/j.jse.2016.11.009
30. Liu X, Joshi SK, Ravishankar B, Laron D, Kim HT, Feeley BT. Upregulation of transforming growth factor-beta signaling in a rat model of rotator cuff tears. J Shoulder Elbow Surg 2014;23:1709-1716. 10.1016/j.jse.2014.02.029
31. Longo GM, Xiong W, Greiner TC, Zhao Y, Fiotti N, Baxter BT. Matrix metalloproteinases 2 and 9 work in concert to produce aortic aneurysms. J Clin Invest 2002;110:625-632. 10.1172/JCI15334
32. Maruyama T, Konkel JE, Zamarron BF, Chen W. The molecular mechanisms of Foxp3 gene regulation. Semin Immunol 2011;23:418-423. 10.1016/j.smim.2011.06.005
33. Matthews TJ, Hand GC, Rees JL, Athanasou NA, Carr AJ. Pathology of the torn rotator cuff tendon. Reduction in potential for repair as tear size increases. J Bone Joint Surg Br 2006;88:489-495. 10.1302/0301-620X.88B4.16845
34. Millar NL, Akbar M, Campbell AL, Reilly JH, Kerr SC, McLean M et al. IL-17A mediates inflammatory and tissue remodelling events in early human tendinopathy. Scientific reports 2016;6:27149. 10.1038/srep27149
35. Navarro P, Trevisan-Herraz M, Bonzon-Kulichenko E, Nunez E, Martinez-Acedo P, Perez-Hernandez D et al. General statistical framework for quantitative proteomics by stable isotope labeling. Journal of proteome research 2014;13:1234-1247. 10.1021/pr4006958
36. Ogata Y, Enghild JJ, Nagase H. Matrix metalloproteinase 3 (stromelysin) activates the precursor for the human matrix metalloproteinase 9. J Biol Chem 1992;267:3581-3584.
37. Opdenakker G, Van den Steen PE, Dubois B, Nelissen I, Van Coillie E, Masure S et al. Gelatinase B functions as regulator and effector in leukocyte biology. J Leukoc Biol 2001;69:851-859.
38. Pasternak B, Aspenberg P. Metalloproteinases and their inhibitors-diagnostic and therapeutic opportunities in orthopedics. Acta Orthop 2009;80:693-703. 10.3109/17453670903448257

627 39. Perez-Riverol Y, Csordas A, Bai J, Bernal-Llinares M, Hewapathirana S, Kundu DJ et al.
628 The PRIDE database and related tools and resources in 2019: improving support for
629 quantification data. Nucleic Acids Res 2019;47:D442-D450. 10.1093/nar/gky1106
630 40. Petersson SJ, Christensen LL, Kristensen JM, Kruse R, Andersen M, Hojlund K. Effect of
631 testosterone on markers of mitochondrial oxidative phosphorylation and lipid metabolism in
632 muscle of aging men with subnormal bioavailable testosterone. Eur J Endocrinol
633 2014;171:77-88. 10.1530/EJE-14-0006
634 41. Reznick AZ, Menashe O, Bar-Shai M, Coleman R, Carmeli E. Expression of matrix
635 metalloproteinases, inhibitor, and acid phosphatase in muscles of immobilized hindlimbs of
636 rats. Muscle & nerve 2003;27:51-59. 10.1002/mus.10277
637 42. Rutella S, Pierelli L, Bonanno G, Sica S, Ameglio F, Capoluongo E et al. Role for
638 granulocyte colony-stimulating factor in the generation of human T regulatory type 1 cells.
639 Blood 2002;100:2562-2571. 10.1182/blood-2001-12-0291
640 43. Sejersen MH, Frost P, Hansen TB, Deutch SR, Svendsen SW. Proteomics perspectives in
641 rotator cuff research: a systematic review of gene expression and protein composition in
642 human tendinopathy. PLoS One 2015;10:e0119974. 10.1371/journal.pone.0119974
643 44. Shannon P, Markiel A, Ozier O, Baliga NS, Wang JT, Ramage D et al. Cytoscape: a
644 software environment for integrated models of biomolecular interaction networks. Genome
645 Res 2003;13:2498-2504. 10.1101/gr.1239303
646 45. Shindle MK, Chen CC, Robertson C, DiTullio AE, Paulus MC, Clinton CM et al. Full-
647 thickness supraspinatus tears are associated with more synovial inflammation and tissue
648 degeneration than partial-thickness tears. J Shoulder Elbow Surg 2011;20:917-927.
649 10.1016/j.jse.2011.02.015
650 46. St Pierre Schneider B, Brickson S, Corr DT, Best T. CD11b+ neutrophils predominate over
651 RAM11+ macrophages in stretch-injured muscle. Muscle & nerve 2002;25:837-844.
652 10.1002/mus.10109
653 47. Toumi H, F'Guyer S, Best TM. The role of neutrophils in injury and repair following muscle
654 stretch. J Anat 2006;208:459-470. 10.1111/j.1469-7580.2006.00543.x
655 48. Yamaguchi K, Ditsios K, Middleton WD, Hildebolt CF, Galatz LM, Teefey SA. The
656 demographic and morphological features of rotator cuff disease. A comparison of
657 asymptomatic and symptomatic shoulders. J Bone Joint Surg Am 2006;88:1699-1704.
658 10.2106/JBJS.E.00835

659 49. Zhao L, Qiu DK, Ma X. Th17 cells: the emerging reciprocal partner of regulatory T cells in
660 the liver. J Dig Dis 2010;11:126-133. 10.1111/j.1751-2980.2010.00428.x
661

Table 1. Cytokine analysis in patients with RC tear.

	SS muscle (pg/mg)	Deltoid muscle (pg/mg)	P-value
IL-1α	2.44 ± 1.38 (n=13)	2.21 ± 1.72 (n=15)	0.83
IL-1Ra	46.83 ± 20.24 (n=14)	34.40 ± 12.94 (n=15)	0.33
IL-2	0.64 ± 0.47 (n=4)	0.41 ± 0.24 (n=5)	0.50
IL-2Ra	93.08 ± 56.28 (n=8)	99.11 ± 76.81 (n=7)	0.87
IL-4	0.04 ± 0.07 (n=6)	0.07 ± 0.08 (n=6)	0.53
IL-9	1.12 ± 0.72 (n=16)	1.10 ± 0.62 (n=17)	0.98
IL-12/IL-23p40	14.35 ± 29.01 (n=15)	14.64 ± 7.71 (n=18)	0.78
IL-12p70	0.23 ± 0.07 (n=6)	0.39 ± 0.32 (n=7)	0.55
IL-13	2.76 ± 2.25 (n=3)	4.35 ± 3.68 (n=3)	0.31
MIF	28,656 ± 18,419 (n=9)	26,617 ± 19,295 (n=8)	0.36
IFN-β	46.08 ± 27.05 (n=8)	34.05 ± 37.80 (n=7)	0.56
IFN-γ	2.23 ± 3.48 (n=5)	2.92 ± 2.11 (n=4)	0.95
FLT3L	14.29 ± 5.13 (n=5)	15.01 ± 8.78 (n=4)	0.93
TRAIL	54.41 ± 23.81 (n=17)	47.00 ± 17.70 (n=19)	0.50
CXCL1/GROα	2.63 ± 2.05 (n=9)	3.92 ± 3.37 (n=8)	0.16
CXCL10/IP-10	8.73 ± 4.00 (n=7)	8.69 ± 2.94 (n=9)	0.86
CXCL11/I-TAC	6.74 ± 2.02 (n=15)	7.78 ± 3.00 (n=19)	0.28
CCL2/MCP1	4.03 ± 2.38 (n=8)	4.83 ± 2.17 (n=9)	0.33
CCL3/MIP-1 α	4.58 ± 2.35 (n=5)	4.01 ± 4.05 (n=2)	-
CCL4/MIP-1β	5.17 ± 1.62 (n=9)	6.35 ± 1.54 (n=8)	0.29
CCL7/MCP-3	4.92 ± 2.59 (n=8)	4.03 ± 3.41 (N=6)	0.33
CCL8/MCP-2	1.52 ± 0.76 (n=8)	1.71 ± 1.11 (n=4)	0.48
CCL13/MCP4	15.64 ± 11.80 (n=8)	9.57 ± 7.33 (n=7)	0.24
CCL17/TARC	3.05 ± 1.01 (n=7)	3.40 ± 0.59 (n=8)	0.41
M-CSF	5.45 ± 3.46 (n=9)	6.27 ± 3.39 (n=6)	0.84
GM-CSF	0.13 ± 0.14 (n=3)	0.10 ± 0.11 (n=7)	0.33
LT-α	1.60 ± 0.79 (n=6)	1.67 ± 0.61 (n=9)	0.41
YKL-40/CHI3L1	121.40 ± 37.64 (n=5)	340.80 ± 274.40 (n=9)	0.18
VEGF-A	93.36 ± 31.19 (n=7)	134.40 ± 53.22 (n=9)	0.19

Paired Student's t-test

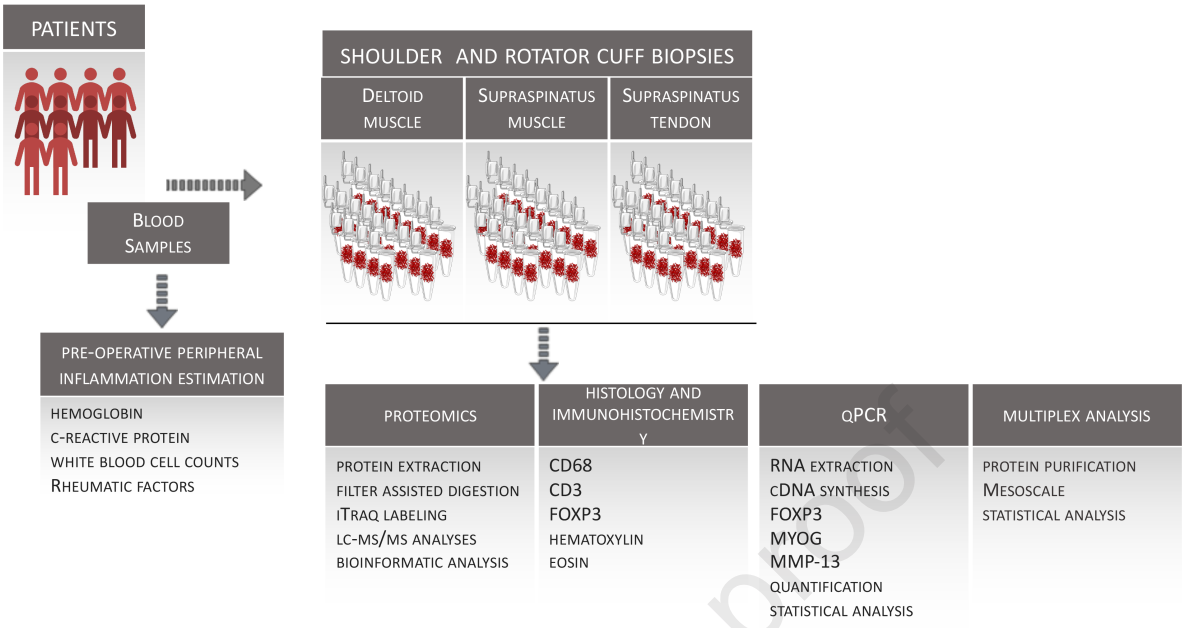

A

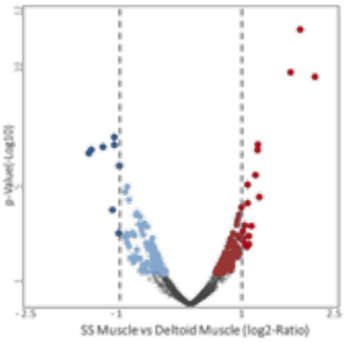

B

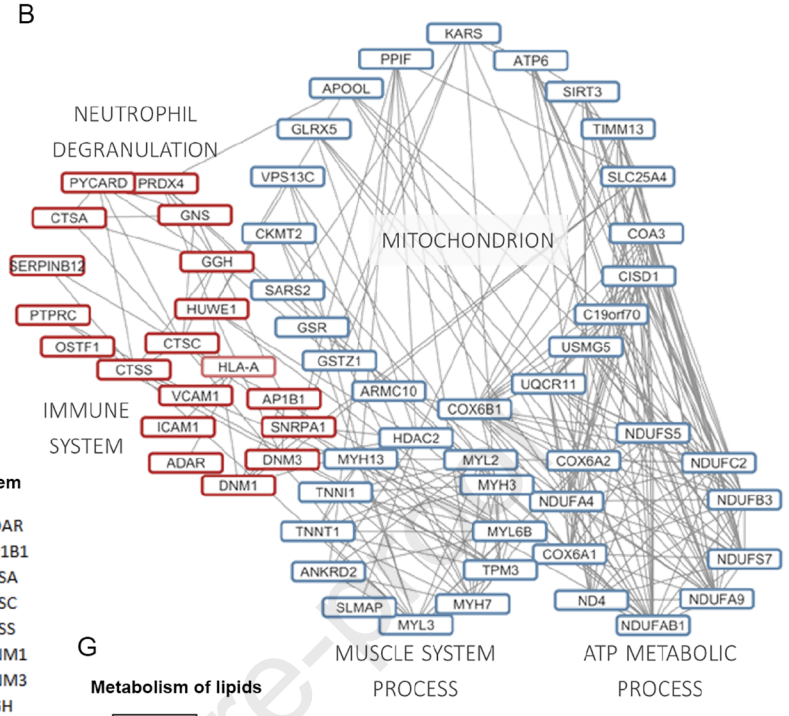

C

Leukocyte mediated immunity

1.62	CTSA
1.83	CTSC
1.74	CTSS
2.06	GGH
1.84	GNS
1.89	HLA-A
1.70	HUWE1
1.73	ICAM1
4.61	OSTF1
1.50	PRDX4
1.68	PTPRC
2.41	PYCARD
1.66	SERPINB12

D

Immune effector process

1.69	ADAR
1.62	CTSA
1.83	CTSC
1.74	CTSS
2.06	GGH
1.84	GNS
1.89	HLA-A
1.70	HUWE1
1.73	ICAM1
1.49	LGALS1
4.61	OSTF1
1.50	PRDX4
1.68	PTPRC
2.41	PYCARD
1.66	SERPINB12

E

Immune system

1.69	ADAR
1.53	AP1B1
1.62	CTSA
1.83	CTSC
1.74	CTSS
1.87	DNM1
1.99	DNM3
2.06	GGH
1.84	GNS
1.89	HLA-A
1.70	HUWE1
1.73	ICAM1
1.64	NUP62
4.61	OSTF1
1.50	PRDX4
1.68	PTPRC
2.41	PYCARD
1.66	SERPINB12
1.90	SNRPA1
1.87	VCAM1

F

Positive regulation of lipid metabolic process

1.39	ADIPOQ
1.05	APOA1
0.83	APOA2
1.12	APOA4
1.11	APOE
1.10	EEF1A2
1.02	F2
1.28	SORBS1

G

Metabolism of lipids

1.62	CTSA
1.59	FABP4
1.62	FASN
4.89	FDXR
1.70	FITM2
2.00	HEXA
2.02	HPGDS
1.52	PLIN1
1.89	PON2
1.79	PPT1
1.81	SACM1L
1.78	SLC25A1

H

Electron transport chain

0.78	ALDH5A1
0.77	COX6A1
0.47	COX6A2
0.82	COX6B1
0.80	GLRX5
0.78	GSR
0.81	ND4
0.77	NDUFA4
0.75	NDUFA9
0.79	NDUFAB1
0.84	NDUFB3
0.50	NDUFC2
0.74	NDUFS5
0.83	NDUFS7
0.72	UQCR11

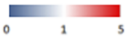

I

Extracellular matrix organization

2.03	CMA1
3.49	COL5A3
1.74	CTSS
2.40	ELN
1.94	ENG
1.55	FBN1
1.73	ICAM1
1.91	MFAP4
2.17	MMP19
1.50	PRDX4
1.87	VCAM1

J

Muscle structure development

0.47	ANKRD1
0.68	ANKRD2
0.72	MYH3
0.79	MYH7
0.78	MYL2
0.76	MYL3
0.76	MYL6B
0.70	MYOZ2
0.69	TNNI1
0.41	UCHL1

K

Striated muscle contraction

0.72	MYH3
0.79	MYH7
0.78	MYL2
0.76	MYL3
0.69	TNNI1
0.75	TNNT1